Tzu Chi Medical Journal 2025; 37 (2): 175-180

Original Article

Rare APOE p.Gly4Glu: A putative disease-causing variant for early-onset Alzheimer's disease identified by next-generation sequencing

Chu-Ting Wu[a,b], Liang-Hsuan Hu[c], Hui-Ying Weng[d], Yen-Ming Liu[e], Yung-Feng Lin[e], Shih-Feng Tsai[e], Raymond Y. Lo[f,g,h], Yung-Hao Ching[c]**

[a]Department of Medicine, Tzu Chi University, Hualien, Taiwan, [b]Department of Family Medicine, Puli Christian Hospital, Nantou, Taiwan, [c]Department of Molecular Biology and Human Genetics, Tzu Chi University, Hualien, Taiwan, [d]Biomedical Industry Ph.D. Program, National Yang Ming Chiao Tung University, Taipei, Taiwan, [e]Institute of Molecular and Genomic Medicine, National Health Research Institute, Miaoli, Taiwan, [f]Department of Neurology, Taitung St. Mary's Hospital, Taitung, Taiwan, [g]Department of Neurology, Hualien Tzu Chi Hospital, Buddhist Tzu Chi Medical Foundation, Hualien, Taiwan, [h]Department of Biochemistry and Molecular Medicine, National Dong Hwa University, Hualien, Taiwan

Submission : 08-May-2024
Revision : 02-Jul-2024
Acceptance : 20-Sep-2024
Web Publication : 07-Apr-2025

Abstract

Objectives: We aimed to identify the early-onset Alzheimer's disease (EOAD)-causing variants in the Eastern Taiwanese population. **Materials and Methods:** Twenty-one patients diagnosed with EOAD in the memory clinic at Hualien Tzu Chi Hospital were enrolled during 2014–2018. We conducted whole-exome sequencing to identify the disease-causing variations and validated by Sanger sequencing. SIFT, PolyPhen-2, and AlphaFold were applied to predict the functional impact of the identified variants. **Results:** Two unrelated normolipidemic EOAD patients were carrying a rare heterozygous *APOE* variant (*rs373985746*, NC_000019.10:g. 44905879*G>A*, NM_001302688.2:c. 11*G>A*, and NP_001289617.1:p.Gly4Glu) with the allele frequency as 0.000206. Sanger sequencing uncovered the ε haplotypes in which the c.11G>A variation resided. SIFT predicted that the variant severely impacts protein structure and, maybe thus, function. AlphaFold predicted a dysfunctional conformation of the mutant APOE precursor a protein (p.Gly4Glu). **Conclusion:** Our data strongly suggest that the rare p.Gly4Glu variant is associated with EOAD but does not cause dyslipidemia.

Keywords: *Allele frequency, Apolipoproteins E, Early-onset Alzheimer disease, Exome sequencing, High-throughput nucleotide sequencing*

Introduction

Alzheimer's disease (AD), one of the most prevalent causes of dementia (60%–80%) [1], is a progressive neurodegenerative disorder associated with cognitive decline. Early-onset Alzheimer's disease (EOAD) is diagnosed in patients under the age of 65 years with more aggressive disease progression and accounts for approximately 5% of AD cases [2,3], while sharing similar pathological features with late-onset AD (LOAD) that include extracellular accumulation of amyloid plaques and intraneuronal accretion of neurofibrillary tangles. Unlike LOAD, genetic variations are the major components of EOAD, with high heritability [4]. EOAD is caused by germline mutations of about 58 candidate genes; among these genes, *amyloid precursor protein* (*APP*), *presenilin 1* (*PSEN1*), and *presenilin 2* only explained 5%–10% of EOAD cases, whereas the remaining 90%–95% remain poorly understood [5]. With the development of next-generation sequencing technologies, such as whole genome sequencing and whole-exome sequencing (WES), clarification of the genetic basis of EOAD has become feasible.

***Address for correspondence:** Dr. Raymond Y. Lo, Department of Neurology, Taitung St. Mary's Hospital, 2, Hangzhou Street, Taitung, Taiwan.
E-mail: raymondlomd@gmail.com
Prof. Yung-Hao Ching, Department of Molecular Biology and Human Genetics, Tzu Chi University, 701, Zhongyang Road, Section 3, Hualien, Taiwan.
E-mail: yching@gms.tcu.edu.tw

How to cite this article: Wu CT, Hu LH, Weng HY, Liu YM, Lin YF, Tsai SF, *et al.* Rare APOE p.Gly4Glu: A putative disease-causing variant for early-onset Alzheimer's disease identified by next-generation sequencing. Tzu Chi Med J 2025;37(2):175-80.

Supplementary material available online

Access this article online

Quick Response Code:

Website: www.tcmjmed.com

DOI: 10.4103/tcmj.tcmj_117_24

The three human *APOE* haplotypes – ε*2*, ε*3,* and ε*4* – defined by two common SNPs (*rs429358* and *rs7412*), with worldwide frequencies of 8.4%, 77.9%, and 13.7%, respectively [6], are the major risk factors of LOAD identified by genome-wide association studies. The ε*3* haplotype is the major allele, and its associated risk of AD is considered a population reference; the ε*4* haplotype is the major risk factor of AD, whereas the ε*2* haplotype exerts a protective effect. Furthermore, the allele frequency of the ε*4* haplotype among EOAD patients was enriched 2.3 times compared to the control population, and carriage of at least one ε*4* haplotype increased the risk of EOAD 3.0-fold compared to subjects without an ε*4* haplotype [7]. In addition, the ε*4* haplotype was associated with earlier onset of AD symptoms in *PSEN1* mutation carriers [8], whereas the ε*2* haplotype delayed the age of onset [9]. We calculated the allele frequency in the Taiwanese population from 280 unaffected individuals participating in the Flagship Program of Precision Medicine for the AsiaPacific, Taiwan National Health Research Institutes. The haplotype frequencies of ε*2*, ε*3,* and ε*4* within the Taiwanese population were 6%, 82%, and 12%, respectively [Supplementary Table S1], comparable to their worldwide frequencies.

In this study, we used WES to identify a rare heterozygous variant, *APOE* (g. 44905879G>A; c. 11G>A; p.Gly4Glu), that was identical in two unrelated EOAD patients. The variant is located at the signal peptide of the APOE precursor protein. In addition, we investigated the ε haplotype that carries the variant. Our data strongly suggest that the rare *APOE* g. 44905879G>A is associated with EOAD.

Materials and methods

Patient recruitment and clinical assessments

The study was approved by the Institutional Review Board of Hualien Tzu Chi Hospital (IRB 106-124-A). Informed consent was obtained from all participants and/or their guardians. This study conformed to the tenets of the Declaration of Helsinki. Twenty-one Taiwanese patients were diagnosed with EOAD in the memory clinic at Hualien Tzu Chi Hospital by a board-certified neurologist with expertise in dementia (R.Y.L.) during 2014–2018. AD was diagnosed according to the National Institute on Aging–Alzheimer's Association criteria [10] supplemented by optional Florbetaben positron emission tomography (PET). EOAD was defined by the onset of the first cognitive symptom before the age of 65 years.

Genomic DNA extraction

Genomic DNA was extracted from peripheral blood. Three ml peripheral blood samples were collected into an EDTA tube (BD Vacutainer TM Cat#367838), followed by inverting the tube several times to prevent coagulation. The blood samples were treated with three volumes of RBC lysis solution (Qiagen, Cat# 158908), inverted to ensure proper mixing, and held at room temperature for five min. The mixtures were centrifuged at 2000 ×*g* for two min to form leukocyte pellets, which were suspended in 600 μL NTES buffer (100 mM NaCl; 50 mM Tris/HCl, pH = 8, 50 mM EDTA), treated with 15 μL of 10 mg/mL proteinase K, and then incubated overnight at 55°C. To extract DNA from other cell components, the mixtures were added to one volume of phenol: chloroform: isoamyl alcohol (25:24:1), vortexed for 10 min, and centrifuged at 12,000 ×*g* for 10 min. The top phase was transferred to a new tube to which 700 μL of 100% isopropanol was added to obtain genomic DNA. Dehydration was accomplished by washing DNA by adding 70% ethanol twice to remove salt followed by the addition of 100% ethanol. Aliquots of 300 μL TE buffer were added to suspend and store DNA. Spectrophotometry (NanoDrop; ThermoFisher Scientific) and fluorometry (Qubit ThermoFisher Scientific) were used to qualify and quantitate genomic DNA with quality of OD260/280 between 1.85 and 1.88. DNA integrity was evaluated by gel electrophoresis on 1% agarose gel. DNA samples were stored at −20°C.

TaqMan allelic discrimination assay

We applied the *TaqMan*® allelic discrimination assay (ThermoFisher, Cat#4351379) according to the manufacturer's instructions to genotype the *APOE* ε allele, comprising two positions, *rs429358* and *rs7412*.

Whole-exome sequencing

All samples underwent WES at the Taiwan National Health Research Institutes. Agilent SureSelect Clinical Research Exome V2 (Agilent, Cat# 5190-9493) was used for whole-exome enrichment. Genomic DNA was fragmented by an enzyme into 150–200 bp, ligated with adaptors, and amplified to prepare a DNA library. The prepared gDNA libraries were hybridized with probes to generate a probe-captured library, and streptavidin-coated magnetic beads captured hybridized DNA. Nonspecific targets were washed out. The captured library was then polymerase chain reaction (PCR) amplified by indexing primers. According to Agilent Technologies, SureSelect probes covered approximately 1100 disease-associated genes, over 75,000 splice sites of noncoding exons, over 12,000 deep intronic variants, over 800 reported variants in promoter regions, and 71 breakpoint spanning probes of common deletions. We used the Illumina NovaSeq 6000 platform, which supports 150 bp paired-end sequencing and a minimum of 100X on-target coverage, to sequence the enriched library. We used CLC Genomics Workbench 12.0.3 software (QIAGEN, Aarhus, Denmark) for raw data analysis, including trimming, read mapping, variant calling, and variant annotation. Adaptors and reads with Phred quality score <20 were trimmed out. Reads were mapped to the human reference genome with mapping length and mapping similarity >0.9. Variant calling was performed only on sequences with over 10 read coverage. dbSNP version 150 (https://www.ncbi.nlm.nih.gov/snp/) and Taiwan Biobank (https://www.twbiobank.org.tw/new_web/) were used to filter out common variants with allele frequencies >1%. The remaining variants were annotated by wANNOVAR.

We conducted candidate gene approaches with the dementia gene panel provided by Blueprint Genetics online, which includes 58 genes.

Sanger sequencing validation

We performed Sanger sequencing to validate the identified variants by WES. We used Primer3 Input (v. 0.4.0) (https://

bioinfo.ut.ee/primer3-0.4.0/) to design primer pairs for the candidate variants. The following primer pairs were designed: (1) for the Patient 13 (P13), forward primer 5'-AAGACCTCTATGCCCCACCT-3', reverse primer 3'-TCGTCCTGAGGTGCTCAACA-5', (2) for the Patient 19 (P19), forward primer 5'-AAAGACCTCTATGCCCCACC-3', reverse primer 3'-GACCTGACCCTACATTCGGT-5'. The primer pairs was synthesized by TAQKEY Science, Taiwan. PCR was performed with a SensoQuest Labcycler. An ABI 3730XL sequencer sequenced PCR products by the Cancer Progression Research Center, National Yang Ming Chiao Tung University. Analysis of sequencing data, including trimming and alignment, was done using Sequencher sequence analysis software.

Haplotyping by TA cloning

The *APOE* ε haplotypes of which the disease-causing variants (*rs373985746*) emerged were identified by PCR amplification of genomic sequence across the variants and the *APOE* haplotype determination SNP *rs429358* and *rs7412*. The amplicons were TA-cloned into *Escherichia coli*; the insert-containing cloning vectors were Sanger sequenced and haplotyped (Mission Biotech, Taiwan).

In silico analysis by SIFT, PolyPhen-2, and AlphaFold

To predict the functional impact of nonsynonymous variants on protein levels, we used SIFT (https://sift.bii.a-star.edu.sg). This algorithm uses sequence conservation and amino acid properties [11] and utilizes PolyPhen-2 (http://genetics.bwh.harvard.edu/pph2/), which employs supervised machine learning and straightforward physical and comparative considerations [12]. PolyPhen-2 uses Bayesian probabilistic models to predict variant effects based on two databases: HumDiv and HumVar. The HumDiv database compares Mendelian disease variants against mammalian orthologues with high sequence identification of a given protein. The HumVar database compares the difference between human disease-causing variations (except cancer mutations) or loss of function variants against common nonsynonymous mutations annotated as benign. We also used AlphaFold [13] to predict the three-dimensional conformational changes of mutant proteins encoded by variants.

Results

Human subjects and clinical presentation

Among the 21 Taiwanese EOAD patients, P13 and P19 called our attention. By WES, we found that P13 and P19 carried a rare identical variant, while other EOAD patients carried unique variants. P13 and P19 are both from Hualien County in Taiwan, and therefore, we conducted haplotyping to determine consanguinity.

This study investigated two nonconsanguineous EOAD patients, P13 and P19. P13 presented with severe memory symptoms and impairment before the age of 66 years. Magnetic resonance imaging (MRI) of the brain at the age of 67 years displayed brain atrophy with prominent cerebral sulci, ventricles, and cisterns [Figure 1a]. P19 experienced short-term memory impairment before the age of 65.

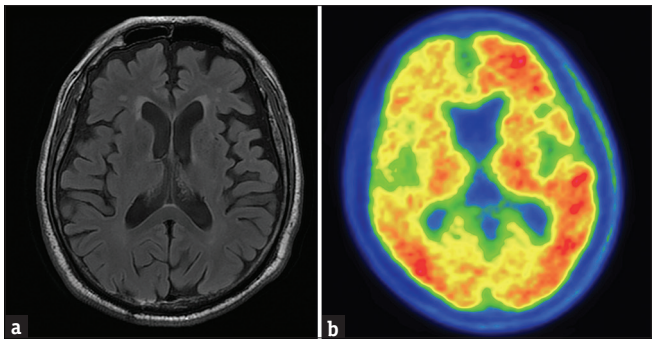

Figure 1: (a) Brain magnetic resonance imaging of P13 at age 67 that shows prominent cerebral sulci, ventricles, and cisterns, indicating brain atrophy. (b) Florbetaben positron emission tomography of P19 at age 70. It shows uptake of Florbetaben, an 18F-labeled polyethylene glycol stilbene derivative with high affinity and specificity for β-amyloid plaques, indicating abnormal brain deposition of β-amyloid plaques

MRI brain scans taken at 65 and 67 years of age showed progressive widening of the sulci, consistent with senile brain atrophy [Supplementary Figure S1]; furthermore, Florbetaben PET at the age of 70 years exhibited abnormal brain deposition of amyloid plaque [Figure 1b]. Both P13 and P19 experienced progressive memory loss with significant declines of CASI and MMSE scores and an increase in CDR [Supplementary Table S2].

In addition, these two EOAD patients were normolipidemic. P13 exhibited a normal value of low-density lipoprotein (LDL) (93 mg/dL, calculated by the Friedewald equation) at age seventy. P19 did not undergo measurement of LDL-C but had no documented history of hyperlipidemia.

Alzheimer risk-related SNPs screening: TaqMan allelic discrimination assay

The TaqMan allelic discrimination assay genotyped the P13 as ε*2*/ε*3*: T/T at *rs429358* and T/C at *rs7412*. The P19 was genotyped as ε*3*/ε*4*: T/C at *rs429358* and C/C at *rs7412* [Figure 2b].

Whole-exome sequencing and allele frequency

Both the P13 and the P19 carried a rare identical heterozygous nonsynonymous variant of *APOE* (NC_000019.10:g.44905879G>A, *rs373985746*) (GRCh38/hg38). The variant g.44905879G>A is located on chr19:44905879; it changes the 11th base from G to A on cDNA (NM_001302688.2:c. 11G>A) and substitutes glutamic acid for glycine at the 4th amino acid of APOE precursor a protein (NP_001289617.1:p.Gly4Glu). The clinical significance and phenotype of the missense mutation were not reported in ClinVar (https://www.ncbi.nlm.nih.gov/clinvar/). This variant has not been reported in Online Mendelian Inheritance in Man (https://www.omim.org). According to 1000 Genomes (www.internationalgenome.org), GnomAD (https://gnomad.broad institute.org), TOPMED, and ExAC (exac.broadinstitute.org), the minor allele frequency for the A allele is $<5 \times 10^{-4}$. According to the Taiwan Biobank (https://taiwanview.twbiobank.org.tw/index), the allele frequency is 0.396%.

Variant validation by Sanger sequencing

We used Sanger sequencing to confirm that the P13 and the P19 carried a heterozygous variant G/A at chr19:44905879 [Figure 2a].

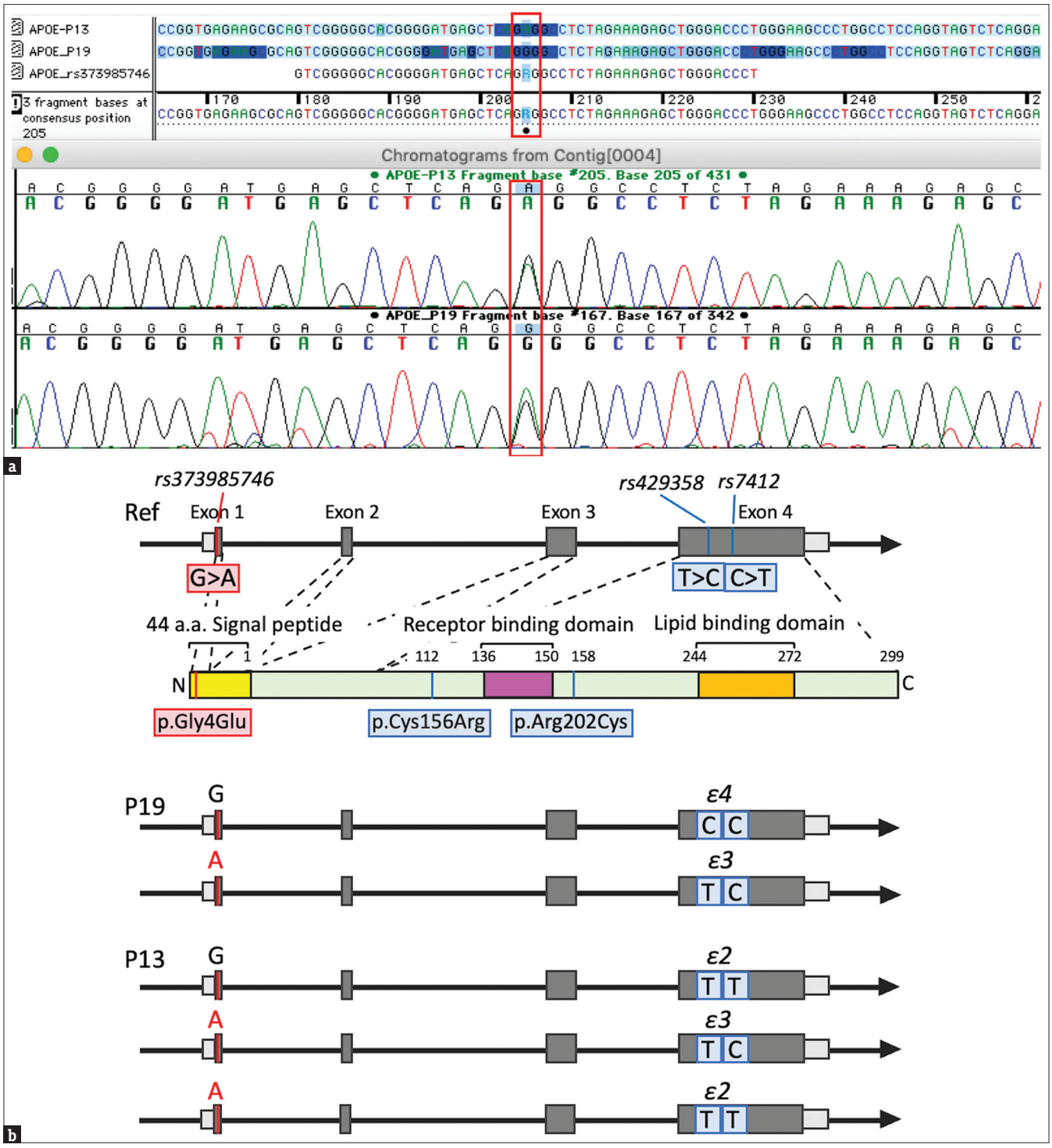

Figure 2: (a) Chromatogram of partial gDNA sequences of the *APOE* gene of P13 (upper row) and P19 (lower row), showing double/heterozygous peaks of A/G at the variant site in *APOE* (NC_000019.10:g.44905879G>A). (b) *APOE* haplotypes of P13 and P19 determined by TA cloning. The schematic drawing shows the merge of the coding sequence and gDNA of *APOE* and its protein product, APOE precursor a (NP_001289617.1). APOE precursor a, composed of 343 amino acids, contains a 44-residue signal peptide, a receptor-binding domain, and a lipid-binding domain. Two single-nucleotide polymorphisms, rs429358 (NC_000019.10:g.44908684T > C, NP_001289617.1:p.Cys156Arg) and rs7412 (NC_000019.10:g.44908822C>T, NP_001289617.1:p.Arg202Cys), determine ε alleles. Three ε alleles (ε2, ε3, ε4) encode APOE protein isoforms which differ at positions 156 and 202. P19 carried ε3/ε4 alleles and g.44905879G>A variant which was *in cis* of *ε3* allele, and *in trans* of *ε4* allele. P13 carried *ε2*/*ε3* alleles but had three different haplotypes: g.44905879G>A variant *in cis* of *ε3* and *ε2* allele, and *in trans* of *ε2* allele. *Ref: Reference, Gly: Glycine, Glu: Glutamate, Cys: Cysteine, Arg: Arginine*

Haplotyping by TA cloning

The P19 carried ε3/ε4 alleles and a g.44905879G>A variant which was *in cis* to the *ε3* allele and *in trans* to the *ε4* allele [Figure 2b]. The P13 carried *ε2*/*ε3* alleles, but through PCR amplification followed by TA cloning, we identified three different haplotypes: the g. 44905879G>A

variant *in cis* to the ε*3* and the ε*2* allele, and *trans* to the ε*2* allele.

In silico analysis: SIFT, PolyPhen-2, and AlphaFold

SIFT predicted that p.Gly4Glu affects protein function with a score of 0.00 due to a lack of inter-species sequence information in the protein family [Supplementary Figure S2]. Therefore, no protein information regarding this site was available. PolyPhen-2 predicted the mutation as unknown on two Bayesian probabilistic models, HumDiv and HumVar, with an unavailable score of damaging probability [Supplementary Figure S3], and found no matches with known protein conformations. Therefore, no information was available regarding this site. By using AlphaFold, the mutant APOE precursor protein (p.Gly4Glu) was predicted to differ from the wild-type; however, it was located within a low-confidence region [Supplementary Figure S4].

Discussion

This study identified a rare APOE variant (*rs373985746*, g.44905879G>A, c.11G>A, p.Gly4Glu) carried by two nonconsanguineous EOAD patients in heterozygous status. The variant was discovered in two unrelated patients, with an allele frequency $<5 \times 10^{-4}$, and arose from two different haplotypes, indicating two independent spontaneous mutation events. To date (March 30th, 2023), 83 *APOE* variants have been reported in ClinVar and primarily cause familial type 3 hyperlipoproteinemia (MIM# 617347). However, the ε*4* allele is associated with LOAD (MIM# 104310). Among reported *APOE* variants, 37 are pathogenic/likely pathogenic, and 13 have unknown clinical significance. None of the pathogenic/possibly pathogenic variants have been associated with EOAD. On the other hand, one *APOE* mutation may protect against EOAD (MIM# 607822). p.Gly4Glu is, to the best of our knowledge, the first reported *APOE* variant that causes the EOAD phenotype.

This study provided the haplotype frequencies of the ε*2*, ε*3*, and ε*4* in the Taiwanese population: 6%, 82%, and 12%, respectively [Supplementary Table S1]. It is comparable to their worldwide frequencies: 8.4%, 77.9%, and 13.7% respectively. The allele frequency was calculated from WES data of 280 unaffected individuals and was kindly provided by the Flagship Program of Precision Medicine for the AsiaPacific, Taiwan National Health Research Institutes.

In silico prediction indicated that the p.Gly4Glu variant is likely to be pathogenic and might severely impact protein structure and, maybe thus, function [Supplementary Figures S2 and S4]. AlphaFold predicted a dysfunctional protein structure of the mutant APOE precursor protein (p.Gly4Glu), especially in the signal peptide region.

The mutation on the signal peptide of APOE (NP_001289617.1) could lead to the failure of APOE secretion, is a possible etiology of EOAD.

The *APOE* gene is located on human chromosome 19q13.32, spanning 3,598 base pairs (chr19:44,905,796-44,909,393) (GRCh38). Five transcripts of *APOE* were observed, which translated into two different APOE precursor proteins: precursor a (NP_001289617.1) and precursor b, composed of 343 and 317 amino acids, respectively. The APOE precursor contains a forty-four residues of signal peptide. The missense mutation g. 44905879G>A, located on the exon 1 of *APOE*, causes the 4th amino acid to change from a small nonpolar glycine (Gly) to a polar glutamic acid (Glu), which is located on the signal peptide of APOE precursor a (NP_001289617.1). The signal sequence specified a particular intracellular destination and was removed by signal peptidase after completing the sorting process [14]; therefore, we speculated that the variation might alter either the final destination of the protein or reduce the cleavage efficacy of peptidase. The protein-targeting route of APOE in the brain cell remains unknown. However, a candidate trafficking route for APOE secretion in macrophages has been proposed: APOE is initially transferred to the endoplasmic reticulum, passed to the Golgi apparatus, and secreted by vesicular transport or recycling endosomes [15]. We speculate that the variant signal sequence might be unrecognized by a complementary sorting receptor that guides APOE to the appropriate organelle, and thereby causes retention of APOE in the cytosol, leading to a deficient level of extracellular functional APOE in the central nervous system (CNS).

The p.Gly4Glu variant leads to EOAD, but might not impact peripheral tissues. In the CNS, functional APOE is produced primarily by astrocytes and microglia and is the main apolipoprotein of HDL [16-19]. In the periphery, APOE is produced primarily by the liver and macrophage [16,17,19], and APOA-1 is the main apolipoprotein of HDL [16]. Mature APOE has two structural domains joined by a hinge region: the receptor-binding region (residue 136–150) in the N-terminal domain and the lipid-binding region (residue 244–272) in the C-terminal domain [17,18]. APOE, which acts as a ligand in receptor-mediated endocytosis of lipoprotein particles, mediates lipid metabolism and participates in the repair of brain injury [16-19]. APOE-mediated neuronal delivery of cholesterol may be required for CNS repair and maintenance of synaptic plasticity [16]. After neuronal secretion, cell-surface ABCA1/ABCG1 lipidates APOE by transferring cholesterol and phospholipid to form lipoprotein particles [18,19]. APOE redistributes cholesterol and lipids through binding to the cell-surface LDL receptor (LDLR) family, including LDLR and LRP1 [16,18].

APOE regulates amyloid β (Aβ) aggregation and clearance and impacts tau phosphorylation and neurotoxicity, synaptic plasticity, and neuroinflammation in an isoform-dependent manner [16,17]. Aβ clearance pathways include cellular uptake, drainage through interstitial fluid or through the blood–brain barrier (BBB), and protease degradation [17,18]. Lipidated APOE binds to soluble Aβ, facilitates cellular uptake of Aβ through LDLR/LRP1/HSPG, and transports Aβ across the BBB [16-18]. Consequently, low APOE levels might impede Aβ cellular uptake, transport, and degradation, thus reducing Aβ clearance. Impaired Aβ clearance promotes Aβ accumulation, forming parenchymal amyloid plaque. APOE deficiency may also exacerbate neuroinflammation, which is implicated in the pathogenesis of AD [16,17] and may be

responsible for poor CNS repair and remodeling capacities under stress or injury.

Our study highlights the role that APOE plays in AD pathogenesis. Two EOAD patients showed cognitive decline, with P19 having amyloid plaque deposition. These two patients were normolipidemic. We hypothesize that p.Gly4Glu decreases extracellular functional APOE in the CNS that consequently leads to EOAD but does not alter lipid levels in the peripheral circulation.

The three *APOE* haplotypes identified in patient P13 are somatic mutations that arose in early embryogenesis or gene duplication. Our study also emphasizes the drawback of the Illumina WES method. p.Gly4Glu might be a somatic mutation that arises during DNA replication and mitosis that is divided into one of the progeny cells. At the same time, the other carries a wild-type allele, resulting in two genetically nonidentical daughter cells during early embryogenesis. The mechanism of gene duplication is not entirely understood. Gene duplication could result from an error of homologous recombination during meiosis or DNA repair. Both of these processes could generate three haplotypes. The gene sequence is uncertain because Illumina NovaSeq 6000 could not identify copy number variations >150 bp, which could be solved by the long-read sequencing method.

A study limitation is the nonavailability of pedigree analysis due to the generation gap of AD. When affected individuals experienced AD onset, their parents were already deceased, while their offspring had not developed symptoms. The lack of *in vitro* or *in vivo* functional analysis is another drawback.

Conclusions

By WES, two unrelated EOAD with normolipidemic patients were identified to carry a rare *APOE* variant (*rs373985746*, NC_000019.10:g.44905879*G>A*, NM_001302688.2:c.11*G>A*, NP_001289617.1:p.Gly4Glu) as heterozygous. The minor allele frequency of the variant is $<5 \times 10^{-4}$. Based on the predicted protein functional impact, our data strongly suggest that the rare p.Gly4Glu variant could be associated with EOAD but does not cause dyslipidemia.

Data availability statement

The datasets generated during and/or analyzed during the current study are available from the corresponding author on reasonable request.

Financial support and sponsorship

This work was supported by the Ministry of Science and Technology (Grant No. MOST-106-2314-B-303 -005), Hualien Tzu Chi Hospital, Buddhist Tzu Chi Medical Foundation, Hualien, Taiwan (Grant No. TCMMP105-08-02, TCRD-105-36, TCRD-106-34, TCRD-107-38).

Conflicts of interest

Dr. Raymond Y. Lo, an editorial board member at *Tzu Chi Medical Journal*, had no role in the peer review process of or decision to publish this article. The other authors declared no conflicts of interest in writing this paper.

References

1. 2022 Alzheimer's Disease Facts and Figures. Alzheimer's Dementia. Alzheimer's Association. 2022, p. 6.
2. Maslow K. Early onset dementia: A national challenge, a future crisis. Washington, DC: Alzheimer's Association; 2006.
3. Prince M, Jackson J. World Alzheimer Report 2009: The Global Prevalence of Dementia. Alzheimer's Disease International. 2009, p. 1-96.
4. Wingo TS, Lah JJ, Levey AI, Cutler DJ. Autosomal recessive causes likely in early-onset Alzheimer disease. Arch Neurol 2012;69:59-64.
5. Cacace R, Sleegers K, Van Broeckhoven C. Molecular genetics of early-onset Alzheimer's disease revisited. Alzheimers Dement 2016;12:733-48.
6. Farrer LA, Cupples LA, Haines JL, Hyman B, Kukull WA, Mayeux R, et al. Effects of age, sex, and ethnicity on the association between apolipoprotein E genotype and Alzheimer disease. A meta-analysis. APOE and Alzheimer disease meta analysis consortium. JAMA 1997;278:1349-56.
7. van Duijn CM, de Knijff P, Cruts M, Wehnert A, Havekes LM, Hofman A, et al. Apolipoprotein E4 allele in a population-based study of early-onset Alzheimer's disease. Nat Genet 1994;7:74-8.
8. Pastor P, Roe CM, Villegas A, Bedoya G, Chakraverty S, García G, et al. Apolipoprotein Eepsilon4 modifies Alzheimer's disease onset in an E280A PS1 kindred. Ann Neurol 2003;54:163-9.
9. Vélez JI, Lopera F, Sepulveda-Falla D, Patel HR, Johar AS, Chuah A, et al. APOE E2 allele delays age of onset in PSEN1 E280A Alzheimer's disease. Mol Psychiatry 2016;21:916-24.
10. McKhann GM, Knopman DS, Chertkow H, Hyman BT, Jack CR Jr., Kawas CH, et al. The diagnosis of dementia due to Alzheimer's disease: Recommendations from the National Institute on aging-Alzheimer's association workgroups on diagnostic guidelines for Alzheimer's disease. Alzheimers Dement 2011;7:263-9.
11. Sim NL, Kumar P, Hu J, Henikoff S, Schneider G, Ng PC. SIFT web server: Predicting effects of amino acid substitutions on proteins. Nucleic Acids Res 2012;40:W452-7.
12. Adzhubei IA, Schmidt S, Peshkin L, Ramensky VE, Gerasimova A, Bork P, et al. A method and server for predicting damaging missense mutations. Nat Methods 2010;7:248-9.
13. Jumper J, Evans R, Pritzel A, Green T, Figurnov M, Ronneberger O, et al. Highly accurate protein structure prediction with AlphaFold. Nature 2021;596:583-9.
14. Alberts B, Johnson A, Lewis J, Raff M, Roberts K, Walter P. Molecular biology of the cell. 6th ed. New York: Garland Science; 2002.
15. Kockx M, Jessup W, Kritharides L. Regulation of endogenous apolipoprotein E secretion by macrophages. Arterioscler Thromb Vasc Biol 2008;28:1060-7.
16. Kim J, Basak JM, Holtzman DM. The role of apolipoprotein E in Alzheimer's disease. Neuron 2009;63:287-303.
17. Liu CC, Liu CC, Kanekiyo T, Xu H, Bu G. Apolipoprotein E and Alzheimer disease: Risk, mechanisms and therapy. Nat Rev Neurol 2013;9:106-18.
18. Yamazaki Y, Zhao N, Caulfield TR, Liu CC, Bu G. Apolipoprotein E and Alzheimer disease: Pathobiology and targeting strategies. Nat Rev Neurol 2019;15:501-18.
19. Flowers SA, Grant OC, Woods RJ, Rebeck GW. O-glycosylation on cerebrospinal fluid and plasma apolipoprotein E differs in the lipid-binding domain. Glycobiology 2020;30:74-85.

Supplementary material

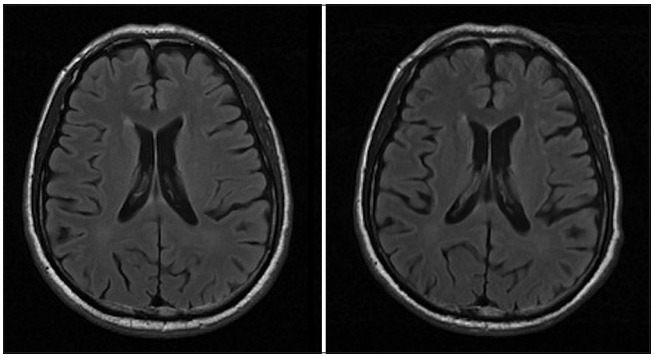

Supplementary Figure S1: Brain magnetic resonance imaging scans of P19 at ages 65 (left) and 67 (right) years. They show senile brain atrophy, a normal variation of sulci widening and aging

a

pos	A	C	D	E	F	G	H	I	K	L	M	N	P	Q	R	S	T	V	W	Y
1M 0.06	0.00	0.00	0.00	0.00	0.00	0.00	0.00	0.00	0.00	0.00	1.00	0.00	0.00	0.00	0.00	0.00	0.00	0.00	0.00	0.00
2S 0.06	0.00	0.00	0.00	0.00	0.00	0.00	0.00	0.00	0.00	0.00	0.00	0.00	0.00	0.00	0.00	1.00	0.00	0.00	0.00	0.00
3S 0.06	0.00	0.00	0.00	0.00	0.00	0.00	0.00	0.00	0.00	0.00	0.00	0.00	0.00	0.00	0.00	1.00	0.00	0.00	0.00	0.00
4G 0.06	0.00	0.00	0.00	0.00	0.00	1.00	0.00	0.00	0.00	0.00	0.00	0.00	0.00	0.00	0.00	0.00	0.00	0.00	0.00	0.00

b

```
          1                                                  50
 QUERY    MSSGASRKSW DPGNPWPPDW PITGRKMKVL WAALLVTFLA GCQAKVEQAV
P02649    XXXXXXXXXX XXXXXXXXXX XXXXXXMKVL WAALLVTFLA GCQAKVEQAV
Q9GLM7    XXXXXXXXXX XXXXXXXXXX XXXXXXMKVL WAALLVTFLA GCQAKVEQVV
Q9GLM8    XXXXXXXXXX XXXXXXXXXX XXXXXXMKVL WAALLVTFLA GCQAKVEQAV
Q9GJU3    XXXXXXXXXX XXXXXXXXXX XXXXXXMKVL WAALLVTFLA GCQAKVEQVV
Q9GLM6    XXXXXXXXXX XXXXXXXXXX XXXXXXMKVL WAALLVTFLA GCQAKVEQAV
P05770    XXXXXXXXXX XXXXXXXXXX XXXXXXMKVL WAALLVTFLA GCQAKVEQPV
P10517    XXXXXXXXXX XXXXXXXXXX XXXXXXMKVL WAALLVTFLA GCQAKVEQPV
Q9GLC0    XXXXXXXXXX XXXXXXXXXX XXXXXXMKVL WAVLAFAFLT GCRADVEPQL
P08226    XXXXXXXXXX XXXXXXXXXX XXXXXXMKAL WAVLLVTLLT GCLA------
Q7M2U7    XXXXXXXXXX XXXXXXXXXX XXXXXXMKVL WAALVVALLA GCWADVELEP
P18650    XXXXXXXXXX XXXXXXXXXX XXXXXXMRVL WVALVVTLLA GCRTEDEPG-
Q03247    XXXXXXXXXX XXXXXXXXXX XXXXXXXXXX XXXXXXXXXX GCQADMEGEL
P23529    XXXXXXXXXX XXXXXXXXXX XXXXXXMKVL WAALVVTLLA GCRADVE---
P02650    XXXXXXXXXX XXXXXXXXXX XXXXXXXXXX XXXXXXXXXT GCLA------
Q7M2U8    XXXXXXXXXX XXXXXXXXXX XXXXXXMKVL WVALVVALLA GCQADMEGEL
P18287    XXXXXXXXXX XXXXXXXXXX XXXXXXMKVW WAVLAAAILA GCRAQTEQEV
P18649    XXXXXXXXXX XXXXXXXXXX XXXXXXXXXX XXXXXXXXXX XXXXXXXXXV
Q28502    XXXXXXXXXX XXXXXXXXXX XXXXXXXXXX XXXXXXXXXX XXXXXXXXXX
Q28995    XXXXXXXXXX XXXXXXXXXX XXXXXXXXXX XXXXXXXXXX XXXXXXXXXX
O42364    XXXXXXXXXX XXXXXXXXXX XXXXXXXXVV FFALAV--LT GCQARLFQA-
P33621    XXXXXXXXXX XXXXXXXXXX XXXXXXXXXX XXXXXXXXXX XXXXXXXXXX
Q28758    XXXXXXXXXX XXXXXXXXXX XXXXXXXXXX XXXXXXXXXX XXXXXXXXXX
P06727    XXXXXXXXXX XXXXXXXXXX XXXXXXXXXX XXXXXXXXXX XXXXXXXXXX
P02651    XXXXXXXXXX XXXXXXXXXX XXXXXXXXXX XXXXXXXXXX XXXXXXXXXX
O46409    XXXXXXXXXX XXXXXXXXXX XXXXXXXXXX XXXXXXXXXX XXXXXXXXXX
```

Supplementary Figure S2: (a) Prediction of tolerance by SIFT. (b) Alignment of APOE orthologues by SIFT

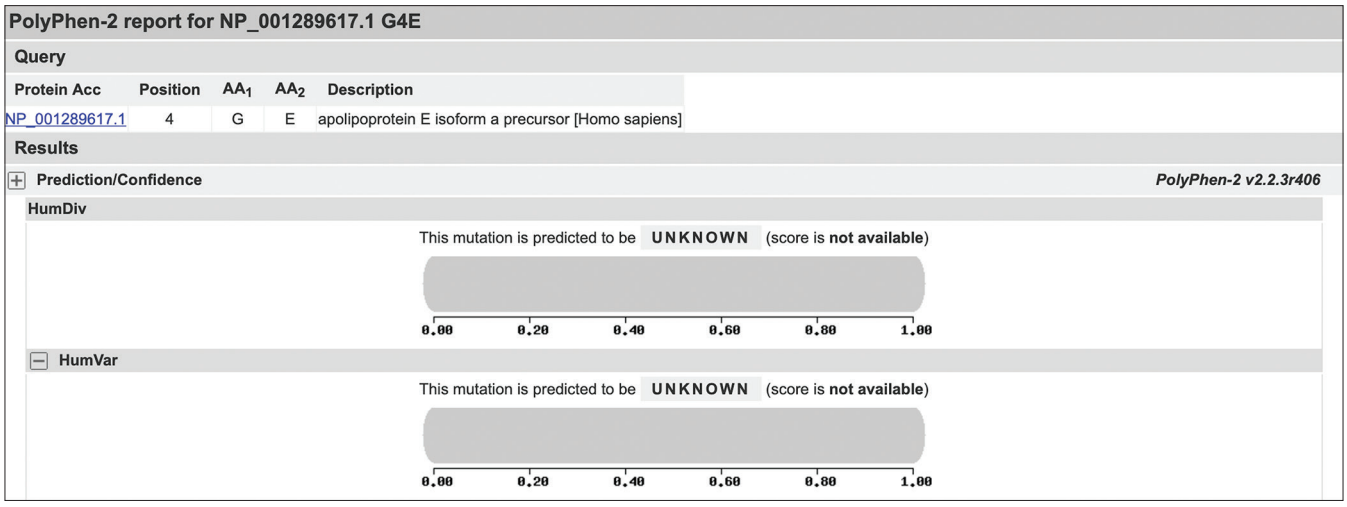

Supplementary Figure S3: Prediction of the p.Gly4Glu by PolyPhen-2. PolyPhen-2 predicted the mutation as unknown on two Bayesian probabilistic models, HumDiv and HumVar. The scores of damaging probabilities of the substitution are not available. G: Glycine, E: glutamate

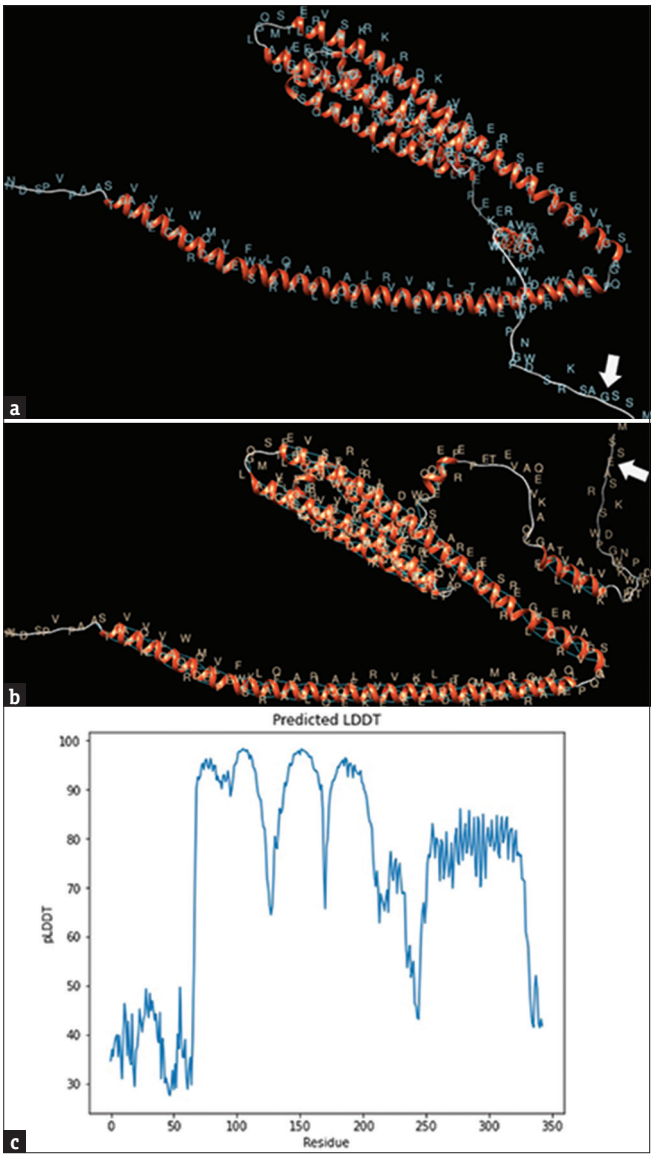

Supplementary Figure S4: (a) Protein structure of wild-type APOE precursor a. (b) Protein structure of mutant APOE precursor a. (c) Per-residue estimate of the confidence

Supplementary Table 1: Allele frequency of ε*2*, ε*3*, and ε*4* in the Taiwanese population

Haplotype	Allele count	Allele frequency (%)
ε*1*	0	0
ε*2*	33	6
ε*3*	458	82
ε*4*	69	12
Number of alleles	560	

Data provided by the Flagship Program of Precision Medicine for the AsiaPacific, Taiwan National Health Research Institutes

Supplementary Table 2: Cognitive test scores of patient 13 (left) and patient 19 (right)

	CASI	MMSE	CDR
Patient 13			
67 years old			
February 12, 2014	83	27	-
August 01, 2014	84	23	1
December 10, 2014	64	19	-
69 years old (February 03, 2016)	56	14	1
70 years old (January 11, 2017)	56	15	1
71 years old (May 16, 2018)	34	9	2
Patient 19			
65 years old (March 30, 2015)	82	23	-
66 years old (March 16, 2016)	74	22	0.5
67 years old (April 06, 2017)	75	23	0.5
68 years old (May 25, 2018)	62	19	0.5
69 years old (June 21, 2019)	56	13	0.5
70 years old (July 24, 2020)	35	12	1

Scores of cognitive tests, including CASI, MMSE, and CDR. CASI and MMSE scores decreased, while that of CDR increased. CASI: Cognitive abilities screening instrument, MMSE: Mini-mental state examination, CDR: Clinical dementia rating scale